RSC Advances

PAPER

View Article Online
View Journal | View Issue

Cite this: *RSC Adv.*, 2016, **6**, 70072

Reduction-controlled substrate release from a polymer nanosphere based on a viologen-cavitand†

Elza D. Sultanova,[ab] Anna A. Atlanderova,[b] Rezeda D. Mukhitova,[a] Vadim V. Salnikov,[cd] Yuriy N. Osin,[c] Albina Y. Ziganshina*[ab] and Alexander I. Konovalov[ab]

Received 11th June 2016
Accepted 19th July 2016

DOI: 10.1039/c6ra15165e

www.rsc.org/advances

In this article, we present a new polymeric nanosphere (p(MVCA-*co*-SS)) for redox-controlled substrate release. The nanosphere consists of a hydrophobic core with disulfide bridges stabilized by the viologen-resorcinarene cavitand shell. The nanosphere is sensitive to thiol-containing reducing agents: glutathione (GSH) and dithiothreitol (DTT). GSH destructs the hydrophobic core of p(MVCA-*co*-SS) while DTT integrates into the core increasing its size. The nanosphere as shown can be used as nanocarriers for the redox-controlled substrate release for the fluorescent dyes (pyrene, rhodamine b and fluorescein).

Introduction

The application field of polymer nanoparticles (PNP) is rapidly expanding.[1–3] PNP have found their place in different areas: in electronics and photonics, in medicine and biotechnology. In recent decades, PNP due to their favorable properties such as good biocompatibility, easy design and preparation, a variety of structures and interesting biomimetic character are widely used as biomaterials.[4–6] In the field of smart drug delivery, PNP play a significant role because they can store and stabilize drugs and effectively deliver them to their target sites.[7–10]

Among the chemically cross-linked polymer particles, widely used ones are disulfide cross-linkers.[11–13] The disulfide bond is a dynamic covalent bond, which can be easily detached and reformed again.[14] Disulfides play an important role in pharmaceutical and biological applications because of their stability under normal conditions and degradation in a reductive environment.[15] Reducing agents such as dithiothreitol (DTT), glutathione (GSH, biologically available) easily cleave the disulfide bonds.[16–19] Chemical reduction of disulfide bonds has been operated for the cellular drug release or cellular imaging.[20,21]

Resorcinarenes are well known class of macrocyclic compounds obtained by the condensation of resorcinol with aldehydes.[22] Resorcinarenes exhibit conformational mobility; however, their flexible macrocyclic structure can be toughened by the intramolecular crosslinking of hydroxyl groups to produce cavitands.[23] The upper rim of cavitands can be easily modified by various groups, so this class of macrocycles is widely used in supramolecular chemistry for the selective binding of various guests. Cavitands have found application in different areas of science mainly in the separation technique[24] and catalysis.[25] Methylviologen cavitands (MVCA, Scheme 1) are redox-active macrocycle consisting four methylviologen groups on the upper rim.[26] MVCA effectively bind multiply charged anions and donors due to the cooperative action of the viologen groups to form host–guest complexes.[27,28] Viologens are 4,4′-bipyridinium salts which can be easily reduced to cation-radical

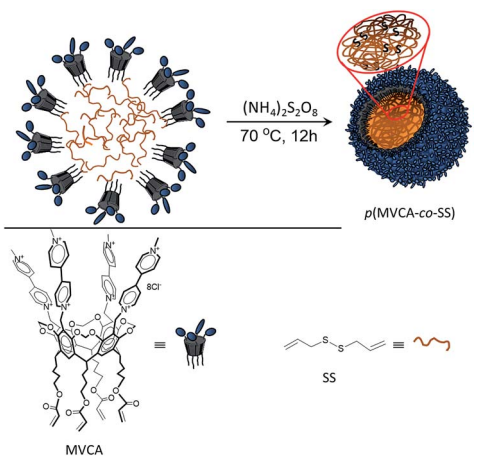

Scheme 1 Synthesis of p(MVCA-*co*-SS).

[a]*Department of Supramolecular Chemistry, A.E. Arbuzov Institute of Organic and Physical Chemistry, Kazan Scientific Center, Russian Academy of Sciences, Arbuzov str. 8, Kazan 420088, Russia. E-mail: az@iopc.ru*

[b]*A.M. Butlerov Institute of Chemistry, Kazan Federal University, Kremlevskaya str. 18, Kazan 420018, Russia*

[c]*Interdisciplinary Center of Analytical Microscopy, Kazan Federal University, Kremlevskaya str. 18, Kazan 420018, Russia*

[d]*Kazan Institute of Biochemistry and Biophysics, Russian Academy of Sciences, Lobachevskii str. 2/31, Kazan 420008, Russia*

† Electronic supplementary information (ESI) available. See DOI: 10.1039/c6ra15165e

and neutral state.[29] Viologens are used as a electroswitchable component in the molecular devices and molecular machines.[30] Viologens show antiviral and antimicrobial activity.[31–33] Multi-viologen can be used in the gene and nucleic acids delivery.[34–36] MVCA reveal amphiphilic properties and self-assembly in aqueous media.[37,38] Earlier, it was demonstrated that MVCA, in a manner similar to cyclodextrins,[39–41] stabilizes o/w emulsions.[42] This behavior was used to creation of the thermosensitive polymeric nanocapsules. The nanocapsules were synthesized by the microemulsion polymerization followed by removing an organic part leaded to the porous and hollow nanocapsules formation. The MVCA-based nanocapsules were applied for the temperature-controlled delivery of hydrophilic species.[42] Work was continued by designing a new nanocarrier, which acts for hydrophobic substrates. For this purpose, a crosslinker with disulfide bonds sensitive to the reducing agents was used in the MVCA polymerization. The crosslinker forms a monolithic core for the hydrophobic species while MVCA cover the core through covalent bonds making the nanocarrier well soluble in water. Herein, we report a synthesis of a core–shell polymer nanoparticle obtained by the polymerization of MVCA (shell component) with diallyl disulfide (core component) and study the possibility of their use in the delivery of hydrophobic substrates.

Results and discussion

The microemulsion polymerization has been applied to obtain monodisperse polymer particles. Diallyl disulfide (SS) represented both as a copolymer of MVCA and an organic part of the microemulsion. SS exhibits two double bonds and its polymerization results in the formation of the branched rigid polymers. A mixing SS (75 mM) with the aqueous solution of MVCA (5 mM) and the ensuing ultrasonic treatment under an argon atmosphere generate an 'oil-in-water' emulsion where SS drops are stabilized with MVCA. Its polymerization results in the formation of the polymer nanoparticles (p(MVCA-*co*-SS), Scheme 1). The polymerization was carried out in 12 h at 70 °C in the presence of the initiator $(NH_4)_2S_2O_8$. After completion of the reaction, p(MVCA-*co*-SS) was isolated, dialyzed for three days to elimination of the initial reagents and being washed with acetone. The size of p(MVCA-*co*-SS) is about 120 nm according to SEM image (Fig. 1). The molecular weight of p(MVCA-*co*-SS) is in the range of 1270 ± 65 kDa, as determined by static light scattering (Fig. S1 in the ESI†). The IR spectrum of p(MVCA-*co*-SS) exhibits the vibration bands of C=O at 1714 cm^{-1} and C=N at 1637 cm^{-1} and the shift and overlay bands of the alkyl and alkene groups at 2800–3100 cm^{-1} (Fig. S2 in the ESI†).

The multi-charged MVCA on the surface of p(MVCA-*co*-SS) make the nanoparticle well soluble and stable in water. $^{13}C\{^1H\}$ NMR spectrum of p(MVCA-*co*-SS) displays the signals of the viologen groups while the resonance signals from the hydrophobic part are dramatically broadened and could not be detected (Fig. 2). In the ^{1}H-NMR spectrum of p(MVCA-*co*-SS), the signals at 5.5–6.0 ppm of the acrylic protons of MVCA completely disappeared, and new broad signals related to the polymerized diallyl disulfide appeared at 1–2.5 ppm, approving the polymerization of MVCA with SS (Fig. S3 in ESI†).

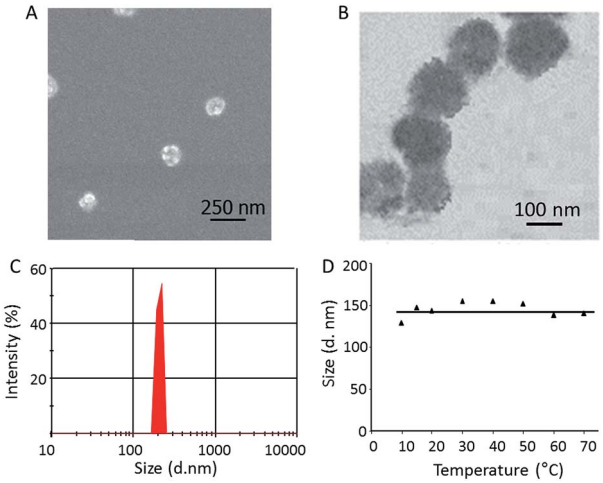

Fig. 1 p(MVCA-*co*-SS): (A) SEM image; (B) TEM image; (C) size distribution diagram determined by DLS and (D) temperature dependence of the hydrodynamic diameter, DLS data (1 mg ml^{-1}, H_2O, 25 °C).

The core–shell structure of p(MVCA-*co*-SS) is confirmed by TEM where the 110–120 nm nanosphere has an amorphous monolithic structure (Fig. 1B). The hydrodynamic diameter of p(MVCA-*co*-SS) is not much larger than its size because of the rigidity of the p(MVCA-*co*-SS) (Fig. 1C). The inflexible structure of p(MVCA-*co*-SS) is approved by the dynamic light scattering (DLS) through a temperature ramping experiment (Fig. 1D). A temperature increase does not affect the size of p(MVCA-*co*-SS) and its hydrodynamic diameter almost does not change.

The hydrophobic core of p(MVCA-*co*-SS) represents an area for the storage of the poorly water-soluble species. It is well illustrated by the examples of the environment-sensitive dyes: pyrene (Py), rhodamine B (RhB) and fluorescein (Fl). The synthesis of p(MVCA-*co*-SS) was carried out in the dye solutions followed by the dialysis for three days at room temperature, results in the nanoparticles with the encapsulated dye (D@p(MVCA-*co*-SS), where D is Py, RhB, Fl). The encapsulated Py exhibits an excimer emission at 470 nm and the decrease of the first emission band at 374 nm (Fig. 3A) indicating the

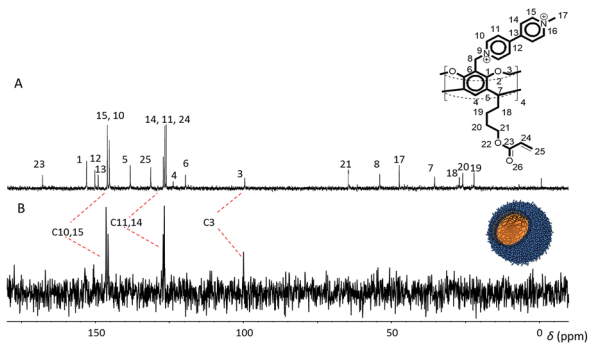

Fig. 2 $^{13}C\{^1H\}$ NMR spectra of (A) MVCA and (B) p(MVCA-*co*-SS) (600 MHz, D_2O).

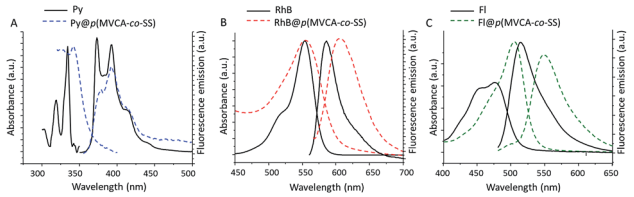

Fig. 3 UV-vis and fluorescence spectra of (A) Py, (B) RhB, (C) Fl in aqueous media and encapsulated into p(MVCA-*co*-SS) (1 mg ml^{-1}, H_2O, 25 °C).

location of the dye in the hydrophobic limited space.[43,44] A significant bathochromic shift, from 580 to 605 nm is observed for RhB inside p(MVCA-*co*-SS) also confirming the organic nature of the SS core (Fig. 3B).[45] Fl@p(MVCA-*co*-SS) displays a greater shift in the emission and absorption peaks in comparison with free Fl (Fig. 3C). It is necessary to note that only the encapsulation into the SS core causes to such significant spectral changes. The cavitand MVCA does not affect qualitatively the dye spectral characteristics. Adding up to ten equivalents of MVCA with pentyl tails to the dyes does not cause to any shift of the spectral bands in the UV and fluorescence spectra (Fig. S4 in ESI†). In the case of Fl, a decrease of the emission intensity without the bands shift appears due to an electron transfer from Fl to viologen moieties (Fig. S4 in ESI†).[46] The nanospheres D@p(MVCA-*co*-SS) are quite stable. There is no release of the dye molecules from the core of p(MVCA-*co*-SS) during their storage at room temperature for more than ten days (Fig. S5 in ESI†).

p(MVCA-*co*-SS) is sensitive to the thiol-reducing agents affecting disulfide bonds. We investigated the changes in p(MVCA-*co*-SS) after the addition of the natural antioxidant glutathione (GSH) and redox reagent with two SH groups – dithiothreitol (DTT). GSH is an important tripeptide performing many biological functions such as neutralization of free radicals and reactive oxygen compounds, regulation of the nitric oxide cycle, involvement in metabolism and in progression of the cell cycle.[47,48] Adding p(MVCA-*co*-SS) (8 mg ml^{-1}) into the water containing 2.5 mg ml^{-1} (8 mM) of GSH causes to the degradation of the polymeric nanospheres. DLS data shows that a distribution peak at 130 nm decreases and multiple peaks in the range 2.5–500 nm appear. Polydispersity index (PDI) increases from 0.29 to 1 (Fig. S6 in ESI†).

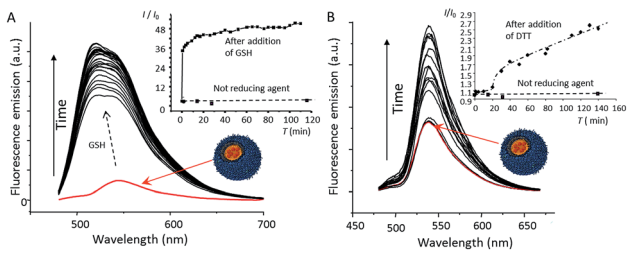

Fig. 4 Fluorescence spectra of Fl@p(MVCA-*co*-SS) (1 mg ml^{-1}) after addition of (A) GSH (0.3 mg ml^{-1}) and (B) DTT (1.2 mg ml^{-1}) (H_2O, 25 °C). (Inset) intensity change at 550 nm in fluorescence spectra of Fl@p(MVCA-*co*-SS) after addition of the reducing agents.

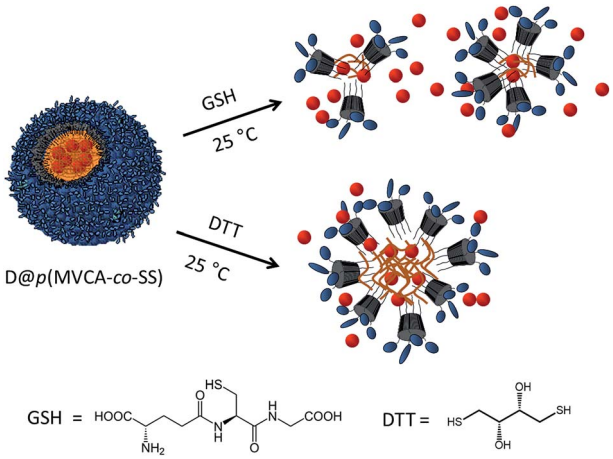

Scheme 2 Redox-controlled dye release from p(MVCA-*co*-SS) under the action of GSH and DTT.

The sensitivity of p(MVCA-*co*-SS) to GSH can be applied in the GSH-controlled species release. The addition of GSH to D@p(MVCA-*co*-SS) causes to the yield the dye molecules to the bulk after the breakdown of the p(MVCA-*co*-SS) core. In fluorescence of Py the first emission peak increases while the excimer band decreases (Fig. S7 in ESI†). In the cases of RhB and Fl the hypsochromic shift of the fluorescence peaks are observed.

The dye yield is the most clearly seen on the Fl, monitoring this action by fluorescence. As shown in Fig. 4A, the emission intensity increases almost 50 times upon at once and the emission peak shifts from 550 to 520, thus confirming the dye release and complete destruction of the SS core. The color of the solution changes from yellow to colorless, indicating the change in the fluorescein environment.

Opposite to GSH, DTT does not completely destroy the hydrophobic core of p(MVCA-*co*-SS). It only changes the size of the cross-linked nanoparticles. According to the DLS data, the addition of 9.3 mg ml^{-1} (60 mM) of DTT leads to an increase of the hydrodynamic size of p(MVCA-*co*-SS) from 130 to 210 nm and a decrease of PDI till 0.01 (Fig. S6 in ESI†). The molecular weight increases slightly to 1320 ± 35 kDa (Fig. S1 in ESI†). Evidently, the DTT influence is more complex. DTT does not only reduces the disulfide bonds, it can embed in the SS core increasing the SS core size and its friability. Therefore, the impact of DTT does not cause the dye out of the cavity (Scheme 2). The addition of DTT to Fl@p(MVCA-*co*-SS) increases the intensity of the fluorescence at three times without the bands shift. This demonstrates that the dye molecules do not yield from the hydrophobic SS core into water. Their motion in the enlarged core is facilitated, leading to enhancement of fluorescence emission of Fl (Fig. 4B).

Experimental

NMR spectroscopic experiments were carried out with an Avance 600 spectrometer (Bruker, Germany) equipped with a pulsed gradient unit capable of producing magnetic-field pulse gradients in the *z* direction of about 56 G cm^{-1}. D_2O

was used as a solvent in all experiments. Chemical shifts were reported relative to HDO ($d = 4.7$ ppm) as an internal standard. UV-vis spectra were recorded with a Perkin-Elmer Lambda 25 UV/vis spectrometer. Fluorescence emission spectra were recorded with a Cary Eclipse fluorescence spectrophotometer (USA). A quartz cell of 1 cm path length was used for all fluorescence measurements. Imaging of the polymer nanoparticles was carried out by intermittent contact mode. Transmission electron microscope (TEM) images were obtained by using JEM-1200EX (JEOL, Japan) instrument at an accelerating voltage of 120 kV. The samples (2–5 μl) were applied on formvar coated copper grids, and then dried at room temperature. The morphology of sample surfaces were characterized in plan-view by scanning electron microscopy (SEM) using high-resolution microscope Merlin Carl Zeiss combined with ASB (Angle Selective Backscattering) and SE InLens (Secondary Electrons Energy selective Backscattering) detectors. A Zetasizer Nano instrument (Malvern, UK) equipped with a 4 mW He:Ne solid-state laser operating at 633 nm was used for SLS and DLS experiments. Malvern dispersion technology software 5.0 was used for the analysis of particle size and molecular weight.

Synthesis of p(MVCA-*co*-SS)

Diallyl disulfide (0.070 ml, 0.5 mmole) was added to a solution of MVCA[42] in water ($C = 5$ mM, $V = 9.7$ ml). The mixture was bubbled with argon for 30 min and then sonicated in the argon atmosphere until the complete homogenization (approximately 80 min). The suspension was heated at 70 °C for 30 min under argon and then ammonium persulfate (20 mg in 0.3 ml water) was added. The suspension heating at 70 °C was continued for 12 h. The final colloidal solution was dialyzed for 3 hour (10 ml *versus* 3 × 800 ml water). Water was removed under reduced pressure. The solid formed was washed with acetone and dried in atmosphere. p(MVCA-*co*-SS) (0.136 g, 80%). Mp > 300 °C. Found: C, 48.89; H, 7,03; N, 2.44. Calc. for $[(C_{108}H_{112}N_8O_{16})\cdot(8Cl^-)\cdot(10C_6H_{10}S_2)\cdot(33H_2O)]_n$: C, 48.99; H, 6,80; N, 2.72%. ν_{max}/cm^{-1} 3100–2900 (CH), 1714 (CO), 1637 (CN). δ_H (600 MHz; D_2O; HDO) 1.2–2.5 (16H, br m, CH_2), 4.1 (8H, br s, CH_2COO), 4.48 (12H, s, CH_3N^+), 5.88 (8H, br s, CH_2N^+), 6.38 (4H, br s, OCH_2O), 7.68 (4H, br s, Ar), 8.5 (16H, br m, N^+CHCH), 9.05 (16H, br m, N^+CHCH), 9.12 ppm (br d, 8H).; δ_C (600 MHz; D_2O) 146.4, 145.4, 127.1, 127.0, 119.8, 99.8.

Synthesis of D@p(MVCA-*co*-SS), where D – Py, RhB or Fl

D@p(MVCA-*co*-SS) were synthesized similarly to p(MVCA-*co*-SS) using an aqueous solution of D (5 mM) instead of water. The final colloidal solutions were dialyzed for 3 days (2 ml *versus* 3 × 800 ml water).

Reduction of p(MVCA-*co*-SS) by GSH

To an aqueous solution of p(MVCA-*co*-SS) ($C = 8$ mg ml^{-1}, $V = 0.5$ ml), a solution of GSH ($C = 8$ mM, $V = 0.5$ ml) was added at room temperature. After 10 min, the particle size was determined by DLS. Reduction of p(MVCA-*co*-SS) by DTT to an aqueous solution of p(MVCA-*co*-SS) ($C = 8$ mg ml^{-1}, $V = 0.5$ ml), a solution of DTT ($C = 60$ mM, $V = 0.5$ ml) was added at room temperature. After 10 min, the particle size was determined by DLS.

Release of fluorescein from Fl@p(MVCA-*co*-SS) by GSH

To a solutions of Fl@p(MVCA-*co*-SS) ($C = 1$ mg ml^{-1}, $V = 3$ ml), 0.9 mg GSH was added and fluorescence emission spectra were recorded at different times (0–140 min).

Release of fluorescein from Fl@p(MVCA-*co*-SS) by DTT

To a solutions of Fl@p(MVCA-*co*-SS) ($C = 1$ mg ml^{-1}, $V = 3$ ml), 3.5 mg DTT was added and fluorescence emission spectra were recorded at different times (0–140 min).

Conclusions

In conclusion, we have prepared a new redox-responsive water-soluble nanosphere with rigid monolithic core by the micro-emulsion polymerization of viologen-resorcinarene cavitand with diallyl disulfide. The nanosphere can be applied for the hydrophobic species storage. The influence of the reducing agents GSH and DTT on the structure, stability and the species release is investigated. It is shown that GSH disrupts the nanospheres resulting in the species release while DTT only reorganizes the nanospheres core (Scheme 2).

Acknowledgements

Elza Sultanova thanks the Haldor Topsøe A/S for PhD scholarship.

Notes and references

1 O. J. Cayre, N. Chagneux and S. Biggs, *Soft Matter*, 2011, **7**, 2211–2234.
2 J. P. Rao and K. E. Geckeler, *Prog. Polym. Sci.*, 2011, **36**, 887–913.
3 K. T. Kim, S. A. Meeuwissen, R. J. M. Nolte and J. C. M. van Hest, *Nanoscale*, 2010, **2**, 844–858.
4 V. Delplace and J. Nicolas, *Nat. Chem.*, 2015, **7**, 771–784.
5 A. Nasir, A. Kausar and A. Younus, *Polym.-Plast. Technol. Eng.*, 2015, **54**, 325–341.
6 A. Kumari, S. K. Yadav and S. C. Yadav, *Colloids Surf., B*, 2010, **75**, 1–18.
7 F. Meng, R. Cheng, Ch. Deng and Zh. Zhong, *Mater. Today*, 2012, **15**, 436–442.
8 M. Huo, J. Yuan, L. Tao and Y. Wei, *Polym. Chem.*, 2014, **5**, 1519–1528.
9 E. Allemann, R. Gurny and E. Doelker, *Eur. J. Pharm. Biopharm.*, 1993, **39**, 173–191.
10 J. Panyam and V. Labhasetwar, *Adv. Drug Delivery Rev.*, 2003, **55**, 329–347.
11 H. De Oliveira, J. Thevenot and S. Lecommandoux, *Wiley Interdiscip. Rev.: Nanomed. Nanobiotechnol.*, 2012, **4**, 525–546.
12 E. Emilitri, E. Ranucci and P. Ferruti, *J. Polym. Sci., Part A: Polym. Chem.*, 2005, **43**, 1404–1416.

13 Y. Li, R. Tong, H. Xia, H. Zhang and J. Xuan, *Chem. Commun.*, 2010, **46**, 7739–7741.
14 E.-K. Bang, M. Lista, G. Sforazzini, N. Sakai and S. Matile, *Chem. Sci.*, 2012, **3**, 1752–1763.
15 Y. Kakizawa, A. Harada and K. Kataoka, *J. Am. Chem. Soc.*, 1999, **121**, 11247–11248.
16 Q. Zhang, N. R. Ko and J. K. Oh, *Chem. Commun.*, 2012, **48**, 7542–7552.
17 C. E. Paulsen and K. S. Carroll, *Chem. Rev.*, 2013, **113**, 4633–4679.
18 A. W. Jackson and D. A. Fulton, *Polym. Chem.*, 2013, **4**, 31–45.
19 J.-H. Ryu, R. T. Chacko, S. Jiwpanich, S. Bickerton, R. P. Babu and S. Thayumanavan, *J. Am. Chem. Soc.*, 2010, **132**, 17227–17235.
20 S. Takae, K. Miyata, M. Oba, T. Ishii, N. Nishiyama, K. Itaka, Y. Yamasaki, H. Koyama and K. Kataoka, *J. Am. Chem. Soc.*, 2008, **130**, 6001–6009.
21 R. Hong, G. Han, J. M. Fernández, B.-J. Kim, N. S. Forbes and V. M. Rotello, *J. Am. Chem. Soc.*, 2006, **128**, 1078–1079.
22 W. Sliwa and C. Kozlowski, *Calixarenes and Resorcinarenes. Synthesis, properties and application*, Wiley-VCH, Weinheim, 2009.
23 D. J. Cram and J. M. Cram, Container Molecules and Their Guests, in *Monographs in Supramolecular Chemistry Series*, ed. J. Fraser Stoddart, The Royal Society of Chemistry, Cambridge, 1997.
24 N. Li, R. G. Harrison and J. D. Lamb, *J. Inclusion Phenom. Macrocyclic Chem.*, 2014, **78**, 39–60.
25 K. Kobayashi and M. Yamanaka, *Chem. Soc. Rev.*, 2015, **44**, 449–466.
26 A. Y. Ziganshina, S. V. Kharlamov, E. Kh. Kazakova, Sh. K. Latypov and A. I. Konovalov, *Mendeleev Commun.*, 2007, **17**, 145–147.
27 G. R. Nasybullina, V. V. Yanilkin, N. V. Nastapova, D. E. Korshin, A. Y. Ziganshina and A. I. Konovalov, *J. Inclusion Phenom. Macrocyclic Chem.*, 2012, **72**, 299–308.
28 V. V. Yanilkin, G. R. Nasybullina, A. Y. Ziganshina, I. R. Nizamiev, M. K. Kadirov, D. E. Korshin and A. I. Konovalov, *Mendeleev Commun.*, 2014, **24**, 108–110.
29 P. M. S. Monk, *The Viologens: Physicochemical Properties, Synthesis and Applications of the Salts of 4,4′-Bipyridine*, John Wiley & Sons, Chichester, 1998.
30 V. Balzani, A. Credi and M. Venturi, *Molecular Devices and Machines – A Journey into the Nano World*, WILEY-VCH, Weinheim, 2003.
31 K. Murugavel, *Polym. Chem.*, 2014, **5**, 5873–5884.
32 S. Asaftei and E. De Clercq, *J. Med. Chem.*, 2010, **53**, 3480–3488.
33 I. Kučera, *Biochim. Biophys. Acta*, 2003, **1557**, 119–124.
34 J. Li, A.-M. Lepadatu, Y. Zhu, M. Ciobanu, Y. Wang, S. C. Asaftei and D. Oupický, *Bioconjugate Chem.*, 2014, **25**, 907–917.
35 A. Szulc, M. Zablocka, Y. Coppel, C. Bijani, W. Dabkowski, M. Bryszewska, B. Klajnert-Maculewicza and J.-P. Majoral, *New J. Chem.*, 2014, **38**, 6212–6222.
36 D. Bongard, W. Bohr, M. Swierczek, T. H. Degefa, L. Waldera and R. Brandtc, *Org. Biomol. Chem.*, 2014, **12**, 9583–9591.
37 R. R. Kashapov, S. V. Kharlamov, E. D. Sultanova, R. K. Mukhitova, Yu. R. Kudryashova, L. Y. Zakharova, A. Y. Ziganshina and A. I. Konovalov, *Chem.–Eur. J.*, 2014, **20**, 14018–14025.
38 V. V. Yanilkin, G. R. Nasybullina, N. V. Nastapova, A. Y. Ziganshina, D. E. Korshin, Y. S. Spiridonova, M. Gruner, W. D. Habicher, A. A. Karasik and A. I. Konovalov, *Electrochim. Acta*, 2013, **111**, 466–473.
39 M. Inoue, K. Hashizaki, H. Taguchi and Y. Saito, *J. Dispersion Sci. Technol.*, 2010, **31**, 1648–1651.
40 B. G. Mathapa and V. N. Paunov, *Phys. Chem. Chem. Phys.*, 2013, **15**, 17903–17914.
41 X. Li, H. Li, Q. Xiao, L. Wang, M. Wang, X. Lu, P. York, S. Shi and J. Zhang, *Phys. Chem. Chem. Phys.*, 2014, **16**, 14059–14069.
42 E. D. Sultanova, E. G. Krasnova, S. V. Kharlamov, G. R. Nasybullina, V. V. Yanilkin, I. R. Nizameev, M. K. Kadirov, R. K. Mukhitova, L. Y. Zakharova, A. Y. Ziganshina and A. I. Konovalov, *ChemPlusChem*, 2015, **80**, 217–222.
43 L. Piñeiro, M. Novo and W. Al-Soufi, *Adv. Colloid Interface Sci.*, 2015, **215**, 1–12.
44 J. Duhamel, *Langmuir*, 2012, **28**, 6527–6538.
45 D. A. Hinckley, P. G. Seybold and D. P. Borris, *Spectrochim. Acta*, 1986, **42**, 747–754.
46 J. R. Lakowicz, *Principles of Fluorescence Spectroscopy*, Springer, New York, 3rd edn, 2006.
47 A. N. Koo, H. J. Lee, S. E. Kim, J. H. Chang, C. Park, C. Kim, J. H. Park and S. C. Lee, *Chem. Commun.*, 2008, **48**, 6570–6572.
48 H. Sies, *Free Radicals Biol. Med.*, 1999, **27**, 916–921.